Sensors and Materials, Vol. 20, No. 2 (2008) 055–069
MYU Tokyo

S & M 0705

Flexible Contact Force Sensing Device Using Metal/Polymer Multilayer Structure for Robotic Applications

Eun-Soo Hwang, Young-Ro Yoon[1], Hyung-Ro Yoon[1],
Tae-Min Shin[1] and Yong-Jun Kim[*]

School of Mechanical Engineering, Yonsei University, 134 Shinchon-dong,
Sodaemoon-gu, Seoul 120-749, Korea
[1]Department of Biomedical Engineering, Yonsei University, 234 Maegi,
Heungup, Wonju, Gangwon 220-710, Korea

(Received June 25, 2007; accepted December 26, 2007)

Key words: contact force, ground reaction force, strain gauge, sensitive skin, tactile

In this paper we propose and demonstrate novel flexible contact force sensing devices for 3-dimensional force measurement. To realize the sensor, polyimide and polydimethylsiloxane are used as a substrate, which makes it flexible. Thin-film metal strain gauges, which are incorporated into the polymer, are used for measuring the three-dimensional contact forces. The force sensor characteristics are evaluated against normal and shear loads. The fabricated force sensor can measure normal loads of up to 4 N. The sensor output signals are saturated against loads over 4 N. Shear loads can be detected by voltage drops in the strain gauges. The device has no fragile structures; therefore, it can be used as a ground reaction force sensor for balance control in humanoid robots. Four force sensors are assembled and placed in the four corners of a robot's sole. By increasing the bump dimensions, the force sensor can measure loads of up to 20 N. When loads are exerted on the sole, the ground reaction force can be measured by these four sensors. The measured forces can be used in the balance control of biped locomotion systems.

1. Introduction

Miniaturized pressure sensors are promising devices for use in many applications such as tire pressure monitoring in automobile systems,[1,2] air pressure monitoring in aerodynamic systems[3] and biomedical applications.[4] The emerging technology of micro-electro-mechanical systems (MEMS) has facilitated research into the development

[*]Corresponding author: e-mail: yjk@yonsei.ac.kr

of various types of miniaturized pressure sensors. Many types of MEMS-based pressure sensors have been developed and are now available. Recently, many researchers have been studying how to apply these micro pressure sensors to robotic systems. In robotic systems, pressure sensors can mainly be used for two applications. One is as a ground reaction force sensing device to assist biped robot balance control[5,6] and the other application is as a contact force sensing, i.e., tactile device for dexterous manipulation and human-robot interactions.[7]

Micro pressure sensors can play a significant role in the balance of a biped locomotion system when it walks on an uneven surface.[5] There are two methods for controlling the balance of biped locomotion systems. One is to consider exchanges of the supporting leg. The biped system can avoid tumbling by exchanging the supporting legs before completely falling flat on the ground, and the locomotion is thus dynamically maintained. The other method follows the zero moment point (ZMP) criterion. The ZMP is a point on level ground where the torque generated by both inertial and gravitational forces is zero. If the ZMP exists under the foot, the locomotion system does not tumble. Thus, the desired motion is planned so that the ZMP criterion is satisfied, and the controller is designed to realize such a desired motion.[5,6,8] The problem with this method occurs when the locomotion system walks on an uneven surface. Because of the unevenness, the biped locomotion system may tumble immediately. To prevent this occurring, the real-time measurement of ground reaction forces is essential for controlling the ZMP so that it remains under the foot in such a case. A force sensor array beneath the sole of a humanoid robots' foot can be used to measure the ground reaction forces.

Contact force sensors for manipulators can be realized as an array of micro pressure sensors. In this application, it is necessary for the sensor to measure three-dimensional (3D) contact forces. The measurement of 3D contact forces is critical for determining the full grasp force/torque and preventing object slipping. The lack of sensors that can measure 3D contact force limits the development of the robotic handling of fragile or irregular objects for many applications including the intelligent service robot.[7]

For such applications, many research groups have used a silicon diaphragm structure with more than four polysilicon piezoresistors.[9–13] For contact force sensors, the sensing device should be mechanically flexible. However, the force sensors developed by a silicon process cannot be made flexible. To make them flexible, the structure requires the incorporation of polyimide layers. Some research groups have used a polyimide layer as a connecting material between silicon diaphragm sensors, while others have mounted silicon diaphragm sensors on flexible printed circuit board (PCB) substrates using conductive epoxy.[11,12] However, these packaging processes are very difficult to realize, which reduces the yield. The silicon-diaphragm-based force sensors generally use piezoresistive sensing methods, which require high-cost equipment such as an ion implanter and low-pressure chemical vapor deposition (LPCVD) equipment for their realization. Therefore, the development of silicon-diaphragm-based force sensor is complex and expensive. To reduce the fabrication cost of force sensors, a polymer-MEMS-based process is used. Various polymer-based force sensors have been reported.[13–16] Basically, two types of sensing schemes, resistive and capacitive, are used for polymer-based force sensors. The capacitive sensing method is very effective for

measuring normal loads; however, it is very difficult to use when measuring shear loads. Therefore, it cannot be used practically for 3D load detection.

In this work we demonstrate a novel, robust, and low-cost flexible force sensor array for assisting the balance of robots and for measuring both normal and shear contact forces on manipulators. For the realization of the sensor, polyimide and polydimethylsiloxane (PDMS) are used as a substrate, which makes it flexible, and thin-film metal strain gauges are used for measuring the 3D contact forces. The device has no fragile structures; therefore, it exhibits good overload behavior. Sensitivity is traded for strength and durability. The sensing principle and fabrication of the proposed device are discussed in detail. We successfully demonstrate the measurement of the normal and shear loads using the proposed flexible contact force sensors.

2. Sensing Principle and Sensor Structure

When a substrate is subjected to surface traction, it experiences stresses for maintaining force equilibrium, and the stresses result in strains by Hooke's law.[17] In many cases, thin diaphragm structures are used to magnify these strains. In our approach, we use the deformation of a polymer substrate, which replaces the deformable diaphragm structure in a rigid silicon substrate. The magnitude of strains in the diaphragm structure is determined by its displacement at the center and its thickness, while the magnitude of strains in our proposed structure is determined by the ductility of the polymer substrate. Figure 1 shows schematic views of the proposed ground reaction force sensor and contact force sensor. The strain sensitive elements, the strain gauges, are embedded in the ductile polymer substrate. A thin metal film is used as the strain gauges. Both the polymer and the thin metal film make the sensor flexible.

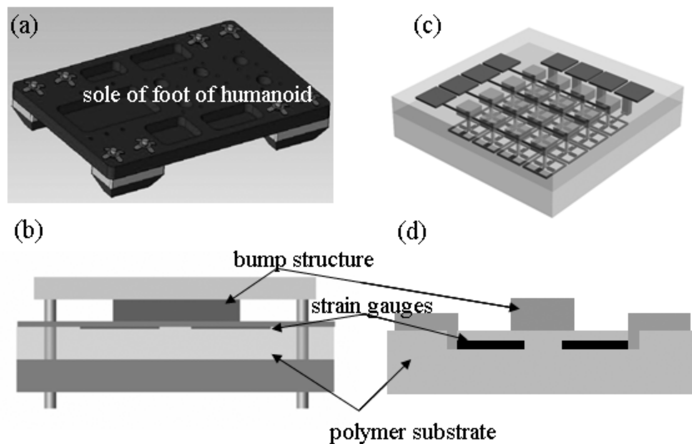

Fig. 1. Schematic views of the proposed contact force sensor array: (a) robot foot sole plate with four ground reaction force sensors, (b) cross-sectional view of one ground reaction force sensor, (c) flexible contact force sensor array for robot manipulator and (d) cross-sectional view of one unit cell.

When an external force is applied onto the device, the polymer and the thin metal film structure deform, which causes a change in resistance. The change in resistance, which corresponds to the applied force, can be measured. The proposed sensor is very stable to overload because it has no fragile structures.

Finite element method (FEM) analysis is used to compare the strains in the polymer substrate and the silicon diaphragm when both are subjected to the same normal load. The dimensions of the silicon diaphragm structure are illustrated in Fig. 2(a) and those of polymer substrate, which has no strain-magnifying structure, are illustrated in Fig. 2(b). For FEM analysis, the material properties of silicon are a Young's modulus of 165 GPa and a Poisson's ratio of 0.22. Those for the polymer substrate are 2.6 GPa and 0.35, respectively. The analysis results are shown in Figs. 2(c) and 2(d). In the case of the silicon diaphragm, the maximum strain is about ten times greater than that of the polymer substrate. However, it can be observed that the strains in the polymer substrate are sufficiently large to be detected using the metal strain gauges. Therefore, the FEM analysis results confirm that the polymer and strain gauges can be used to measure the external load even though they have no strain-magnifying structures.

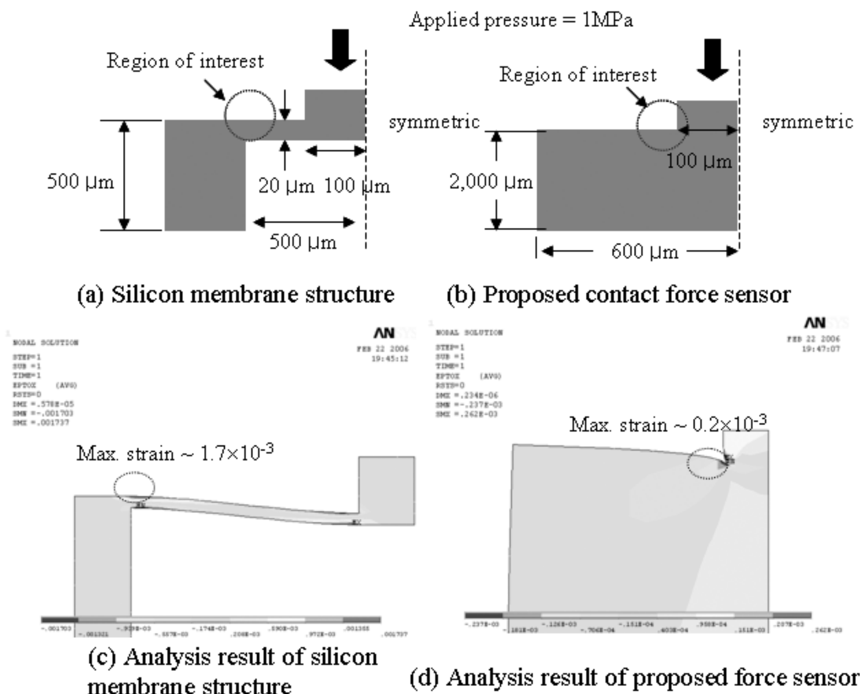

Fig. 2. FEM analysis models and results: (a) dimensions of silicon diaphragm model, (b) dimensions of proposed force sensor model, (c) FEM strain analysis result for silicon diaphragm model and (d) FEM strain analysis result for proposed force sensor model.

Most silicon-diaphragm-based force sensors use doped silicon piezoresistors as the strain gauge material because doped silicon has a very high gauge factor in comparison with other materials. In our work, the doped silicon is not compatible with the polymer substrate. Thus, we can use only thin-film metal as the strain gauge material. The sensitivity of the proposed force sensor is expected to be smaller than that of the silicon diaphragm sensor due to the relatively small strains in the polymer substrate and the low gauge factor of thin film metal gauge. However, the sensor is expected to have a much wider operational force range and good overload behavior. It should also be taken into account that a contact force sensor for robotic application must serve as a barrier against chemical and mechanical contact as well as a source of physical contact information.(13) Therefore, the polymer substrate with thin-film metal strain gauges is a suitable robot skin for both the sole of the foot and the manipulators.

The normal and shear load sensing principles are described in Fig. 3. The four strain gauges are embedded at the center of the ductile polymer substrate. When a normal load is applied to the surface of the sensor, the substrate experiences a deformation. This deformation of the polymer induces an equal strain on both strain gauges, as shown in Fig. 3(a). When a shear load is applied as shown in Fig 3(b), one strain gauge experiences tensile strain and the other one experiences compressive strain. This difference will result in a different voltage drop across each strain gauge. Thus, the shear load can be detected from this voltage drop difference. An unknown load can be measured by the superposition of these two cases.(17) In accordance with these sensing principles, we design the force sensor unit cell to consist of four strain gauges to detect shear load in the *x* and *y* directions.

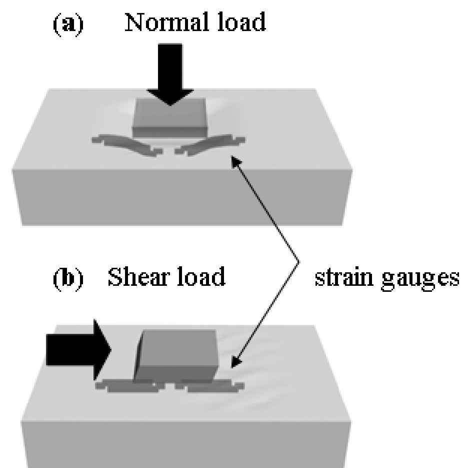

Fig. 3. Normal and shear load sensing principles: (a) in the case of normal load, both strain gauges are subjected to tensile stress and (b) in the case of shear load, one strain gauge is subjected to tensile stress and other is subjected to compressive stress.

3. Fabrication

Figure 4 shows the fabrication steps for the realization of the flexible contact force array. We start the fabrication with a 4 inch oxidized silicon wafer. The oxide thickness is 1 μm. A polyimide (PI) precursor (PI2611 HD MicroSystems) is spin-coated at 1000 rpm and cured at 300°C in a convection oven. This layer is named as the first PI layer. Then a Cu-Ni metal layer is deposited by thermal evaporation to form a 2000 Å thick film and is patterned by wet etching. Figure 4(a) shows the patterned strain gauge array on the hard-cured PI film. The wafer is then coated with a second PI layer and cured. The same conditions as those for the first PI layer are used. The patterned strain gauges are buried between the first and second PI film layers. It has been shown experimentally that the adhesion between metal and PI degrades after 10^8 cycles of mechanical vibration.[18] Burying the strain gauges between the PI layers enhances the adhesion. Thus, the strain gauges in the polymer will be mechanically stable for a long operation period. Next, via holes are formed by reactive ion etching (RIE) using O_2 plasma. Aluminum (Al) is used as a masking layer. After the formation of via holes, a Cr/Cu seed layer is deposited. Then, positive photoresist (AZ7220, Clariant) is spin-coated and patterned to allow selective electroplating. The electroplated Cu interconnection lines are 2 μm thick. This thickness is ten times greater than that of the strain gauge pattern to reduce the resistance in interconnection lines. After this step, Cu electroplating is carried out to form the contact pads and interconnects at one end of the strain gauge, as shown in

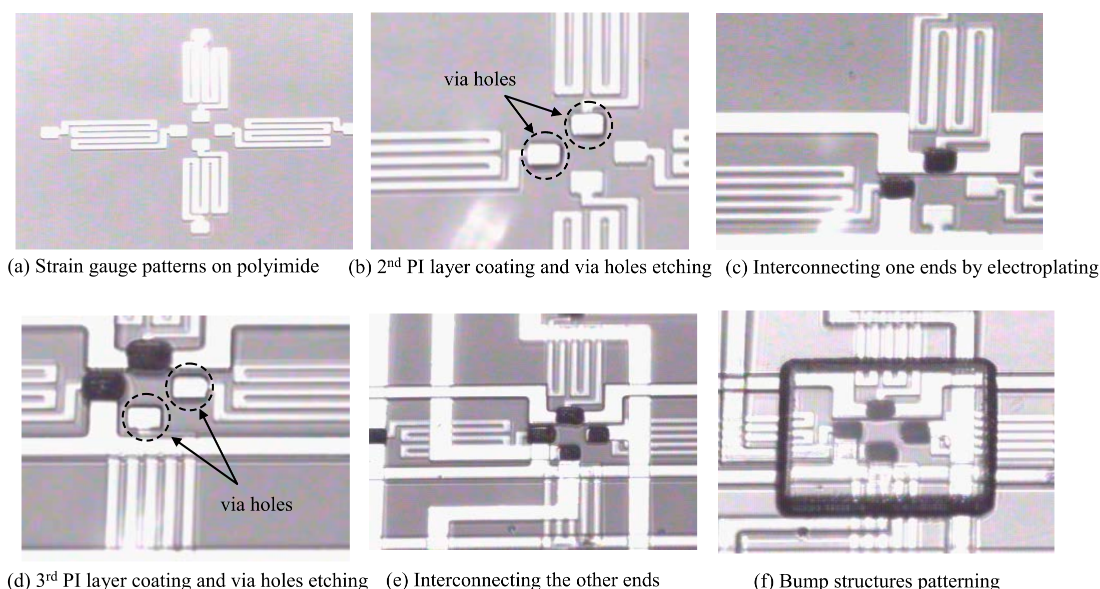

Fig. 4. Fabrication steps for the realization of proposed device.

Fig. 4(c). Thereafter, the wafer is coated with a third PI layer. Then, the same RIE and electroplating processes are employed to form the contact pads and interconnects at the other end of the strain gauge, as shown in Figs. 4(d) and 4(e). After the wafer is coated with a fourth PI layer to insulate the interconnects, the contact pads are selectively opened by RIE. Then, SU8-2050 (MicroChem) bump structures are formed for load concentration, as shown in Fig. 4(f). The bump height is about 50 μm. Finally, the sensor array is released from the silicon wafer by etching out the silicon dioxide layer. Contrary to the concern that the PI would curl and deform the device, no curling is observed.

Figure 5(a) shows photographs of the fabricated flexible contact force sensor array (35×35 mm^2, 70 μm thick). It has 8×8 unit cells and each cell consists of four strain gauges for detecting both normal and shear loads in the *x* and *y* directions. Figure 5(b) shows a close-up view of one unit cell, showing the four strain gauges. The flexibility of the fabricated sensor array is demonstrated in Fig. 5(c) by bending it using fingertips. The fabricated sensors were attached on a ductile PDMS (Sylgard 184, DOW Corning) substrate using 80-μm-thick double-sided adhesive Kapton film. This PDMS substrate plays a significant role in contact force sensing by transforming the applied load into strain.

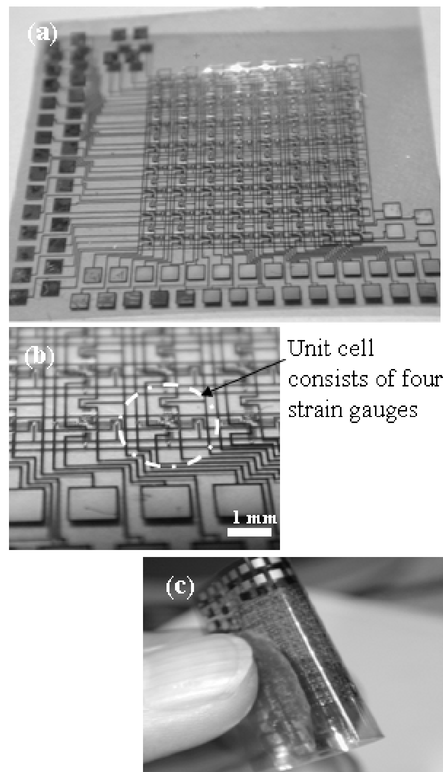

Fig. 5. Photographs of fabricated contact force sensor array for robot manipulators: (a) 8×8 force sensor array (35×35 mm^2 and 70 μm thick), (b) one unit cell consists of four strain gauges for normal and shear load detection in *x* and *y* directions, and (c) sensor, indicating its flexibility.

4. Measurement

The gauge factor, which is defined as the ratio of resistance change rate to applied strain, of the metal strain gauges is measured. The strain gauge is attached on one end of a cantilever and a known force is applied at the other end of the cantilever using a scale weight. The strain can be calculated from the moment-curvature equations, in which the curvature of the cantilever is directly proportional to the bending moment and inversely proportional to the flexural rigidity of the beam.(19) The resistance change rate can be calculated from the measured resistance using semiconductor characterizing system (Keithley 4200). Figure 6 shows the graph of the resistance change rate versus strain. The gradient of the linear graph indicates the gauge factor of the metal strain gauge. The measured gauge factor, 1.81, is in good accordance with a previously reported result.(20) The strain loss in the polymer substrate is negligible.(21)

The unit cell characteristics against normal and shear loads are evaluated. Loads are applied on a unit cell using a load cell. The applied loads are monitored using a load-cell indicator. Voltage drops across each resistor in one unit cell are measured by an analog-to-digital converter (ADC) using a Wheatstone bridge configuration and a voltage amplifier. Using a microprocessor chip (ATMega128), which has 10-bit ADCs, multiplexers for addressing 8×8 sensors, an op-amp for voltage amplification and an RS232C chip, the measured contact information is converted to a digital signal and transmitted to a computer.

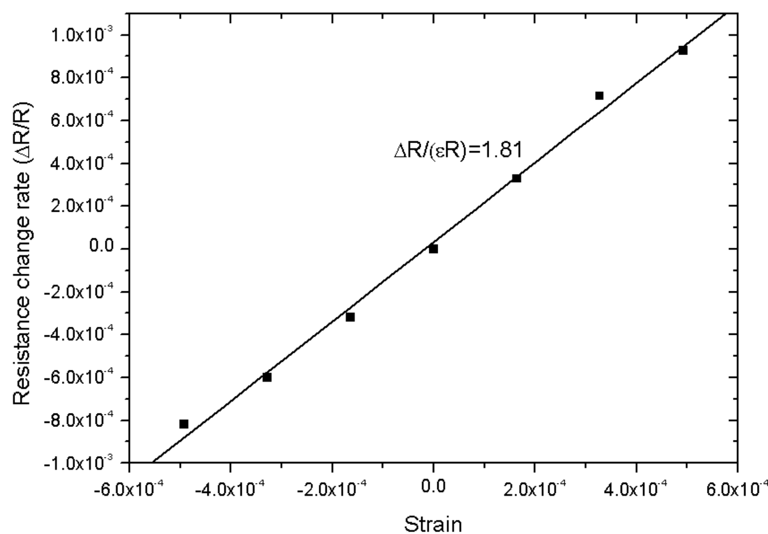

Fig. 6. Graph of the resistance change rate versus applied strain. The gradient of the graph indicates the gauge factor of the fabricated strain gauges.

Figure 7(a) exhibits the normal load measurement result. The voltage drop across the strain gauges is linear with applied normal load. However, the sensitivity is less than that of a diaphragm-based force sensor. The operational load range is from 0 to 4 N. The output signal of the sensor becomes saturated when the applied load is more than 4 N.

According to rubber elasticity theory, a force on a polymer material results in polymer chain extension. The state of a polymer chain extending to its full length is known as polymer chain locking. This polymer chain locking prevents the polymer deformation of over a certain degree.[22] When a polymer sample is under uniaxial

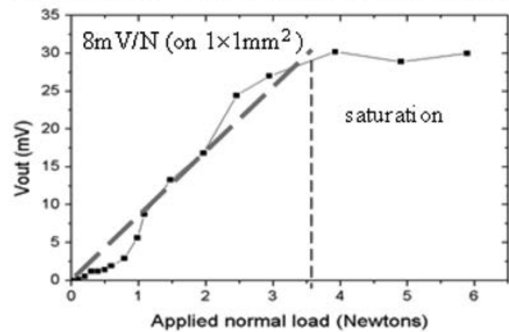

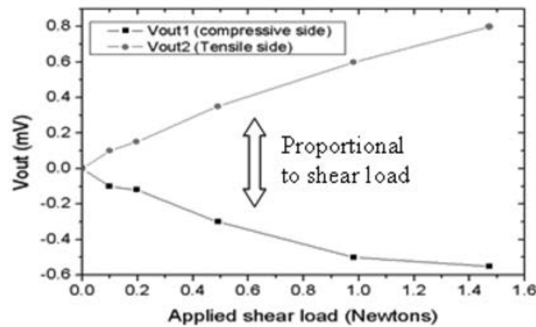

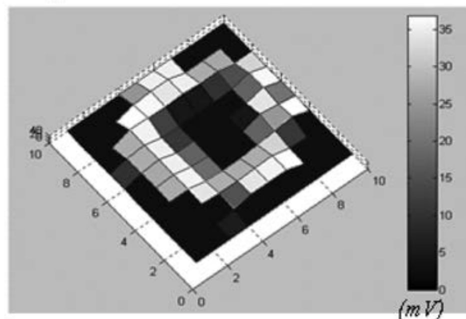

Fig. 7. Measurement results: (a) output voltage versus normal load, (b) output voltage versus shear load and (c) 2D image of test result when sensor array is pressed by ring-shaped object (1 N).

compression, the polymer chains are compressed in the direction of the force but are extended in the two perpendicular directions to the force due to the incompressibility of the polymer substrate (i.e., no volume change).[22,23] Therefore, to an extent, the polymer material is deformed due to this compressive force and the deformation is saturated due to chain locking in the polymer chains. The PDMS polymer substrate that is used in our experiment is deformed by a normal force. At 4 N normal load, which is equivalent to 3.7 MPa pressure, the PDMS substrate deformation was saturated. This result is in agreement with the theoretically expected stress-strain characteristic of PDMS from polymer chain theory.[24]

A pure shear load is applied using adhesive tape by setting up the sensor vertically by attaching it to a rigid object. The shear load test results are shown in Fig. 7(b). It can be observed that the voltage drop across one strain gauge is increasing while that across the other is decreasing as shear load increases. A 2D image test is performed using the 8 ×8 flexible force sensor array. A ring-shaped object of 1 N load is applied to the sensor array. The resulting image is shown in Fig. 7(c). In this image test, the shear signal is very small compared with the normal load signal.

The operational force range of ground reaction force sensor should be larger than that of the contact force sensor for manipulators, which have an operational force range from 0 to 4 N. Our humanoid robot has a mass of about 8 kg. The expected load on one sole of a robot foot is about 80 N when it walks. Since we designed four ground reaction force sensors for one foot sole plate, one contact force cell for sensing ground reaction force should be able to measure loads of up to 20 N. Our approach in this study is to change the bump size to reduce the contact pressure and change the polymer thickness of the fabricated force sensor, since the bump plays a significant role in distributing the applied contact load.

We performed simple experiments by changing the bump size and the polymer thickness to determine the effect of the bump size and the substrate thickness on the sensitivity and maximum detectable load. In this experiment, the bump size was varied from 3×3 mm^2 to 6×6 mm^2 with an increment of 1 mm, and the thickness of the polymer was varied from 1.5 to 5.0 mm. Figure 8 shows the test results for various bump sizes and polymer thicknesses. As shown in Fig. 8(a), the sensitivity can be modified by changing the bump size. The resistance change rate increases when we use a smaller bump size, and this results in a smaller maximum detectable load. The polymer thickness also affects the resistance change rate and maximum detectable load, as shown in Fig. 8(b). It is clear that the sensitivity increases in a thicker polymer substrate, and that the resistance change rate becomes more easily saturated in a thinner polymer substrate.

For the ground reaction force sensor unit cell, a bump size of 4×4 mm^2 and a polymer thickness of 5 mm are used. The ground reaction force sensor structure is the same as that of the fabricated contact force sensor array except for its dimensions, bump size, and polymer thickness. Four force sensor cells are attached at the corners beneath the robot foot sole plate with a front barrier structure. When a humanoid robot stands on the ground or walks, the sensor can measure the ground reaction force immediately. The assembled sensor module is shown in Fig. 9. The ground reaction forces are measured at the four corners of the sole plate. The bump is pressed by the front barrier structure and the deformation of the polymer can be detected by the strain gauges.

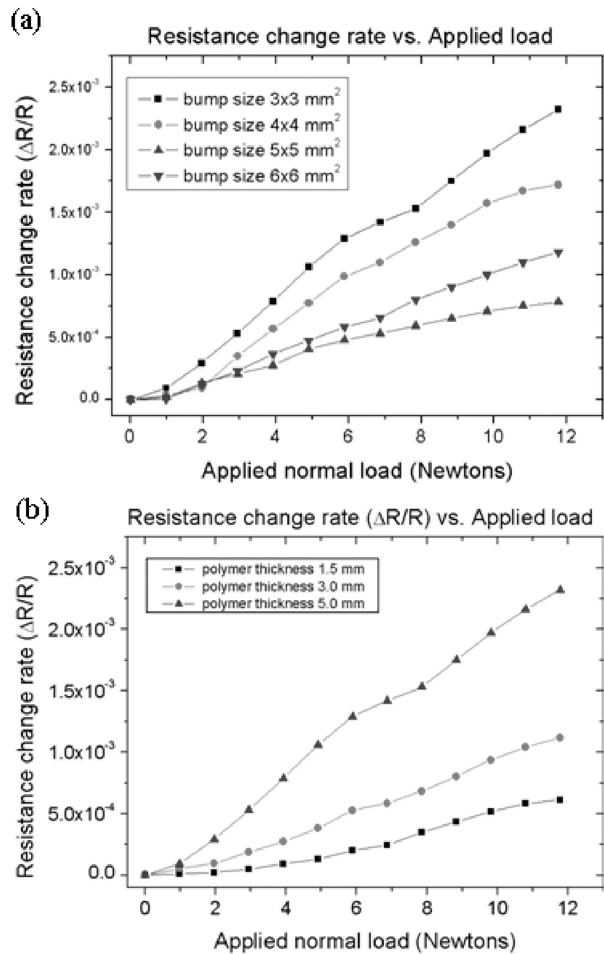

Fig. 8. (a) Graph of the resistance change rate versus the applied load for different bump sizes and (b) graph of the resistance change rate versus the applied load when different polymer thicknesses were used.

We measured the performance of each cell of the ground reaction force sensor. The load is applied at the front barrier structure. The measured resistance changes are processed and sent to the main controllers. Figure 10 shows the result of each cell load test. Each cell can measure a load of up to 20 N within an error of 25%. The full ground reaction force on the robot foot was also measured when the load was applied on the sole plate (as shown in Fig. 11). The results are listed in Table 1. Various loads are applied at the geometrical center of the robot foot plate, as shown in Figs. 11(a)–11(c). In each case, the ground reaction force sensor module can measure the overall load on the robot

foot plate. The measured values at each cell are listed in rows (a)–(c) of Table 1. When a distributed 40 N load is applied on the plate, the sensor can also detect the load, as shown in row (d) of Table 1. When the load is applied on the front part and the rear part of the robot foot plate, the ground reaction force sensor module can detect the center of

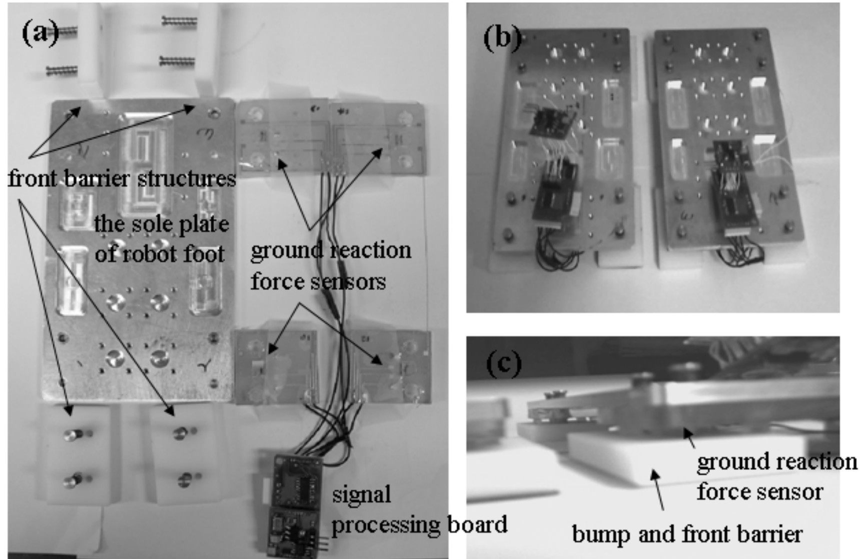

Fig. 9. (a) Parts of ground reaction force sensor and (b) and (c) assembled ground reaction force sensor.

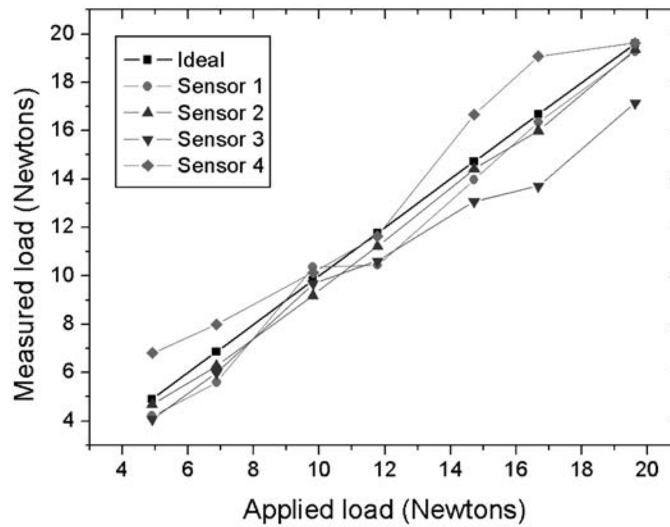

Fig. 10. Graph of sensor signal output versus applied load for ground reaction force sensors.

Table 1
The results of ground reaction force measurement.

	#1	#2	#3	#4	SUM
(a) Applying concentrated load (20 N) at the geometrical center of plate	5.51	7.57	8.10	6.08	27.26
(b) Applying concentrated load (30 N) at the geometrical center of plate	7.69	9.57	8.57	8.52	34.35
(c) Applying concentrated load (40 N) at the geometrical center of plate	9.22	10.16	12.60	9.69	41.67
(d) Applying distributed load (10-20-10 N) along the center line of plate	10.59	8.95	13.73	9.52	42.79
(e) Applying concentrated load (40 N) at the front part of the plate	5.54	6.68	16.97	13.17	42.36
(f) Applying concentrated load (40 N) at the rear part of the plate	13.81	13.93	7.90	8.00	43.64

(Unit: N)

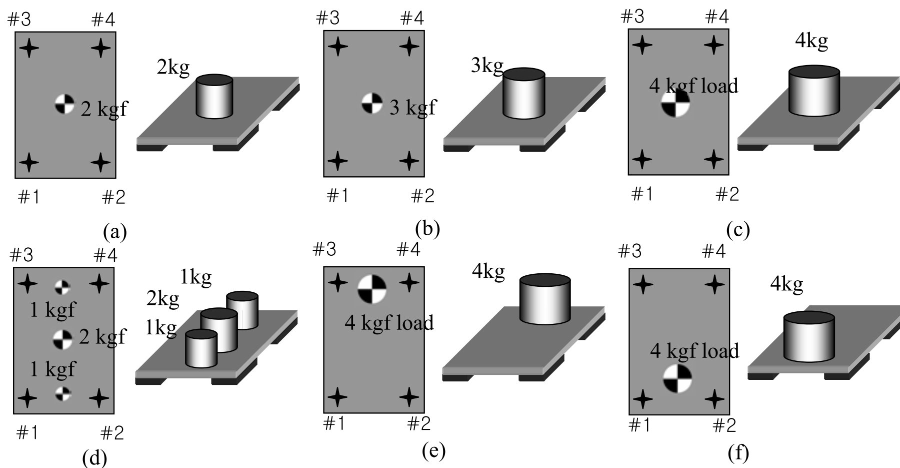

Fig. 11. Measurement of ground reaction force using the proposed ground reaction force sensor module.

pressure, as shown in rows (e) and (f) of Table 1. These measured values can be used for the balance control of a biped locomotion system. In these experiments, the results include some errors. These are due to the rolling effect of the front barrier structure.

5. Conclusion

Novel contact force sensing devices for robotic applications have been proposed and demonstrated. The sensor uses the principle that when a surface is subjected to a load, it experiences stress, which results in strain. By using strain gauges, which are incorporated in a polymer, the strain induced in the polymer substrate can be detected. The measurement results show that the flexible contact force sensor array has lower sensitivity and a wider operational force range than a conventional silicon-membrane-based tactile sensor. The shear load can also be easily detected using a simple measurement circuit.

Since the proposed sensor has a wide operational force range and has no fragile structures it can be used as a ground reaction force sensor. Each cell can measure a load of up to 20 N by modifying the bump size and polymer thickness. Using four force sensor cells, the center of pressure in the humanoid robot foot plate can be detected within a 25% error.

The proposed devices have many advantages: they have a simple fabrication process, overload tolerance, high flexibility, and durability. However, they have relatively low sensitivity and are inaccurate for the measurement of a small load. The most promising aspect of the devices is the simultaneous detection of normal and shear loads using a simple structure. This sensor can be used as a sensitive robot skin due to its robustness and wide operational force range.

Acknowledgement

This study was supported by a grant from the Korea Health 21 R&D Project, Ministry of Health & Welfare, Republic of Korea (Grant A020602).

References

1 M. Kowalewski: IEEE Potentials **23** (2004) 8.
2 W. Tjiu, A. Ahanchian and B. Y. Majlis: Proc. IEEE Int. Conf. Semiconductor Electronics (Kuala Lumpur, 2004) p. 350.
3 S. Callegari, M. Zamoni, A. Golfarelli, M. Tartagni, A. Talamelli, P. Proli and A. Rossetti: Sens. Actuators A **130–131** (2006) 155.
4 K. J. Rebello: Proc. IEEE **92** (2004) 43.
5 P. Sardain and G. Bessonnet: IEEE Trans. Systems, Man and Cybernetics Part A: System and Human **34** (2004) 638.
6 S. Kagami, Y. Takahashi, K. Nishiwaki, M. Mochimaru and H. Mizoguchi: Proc. IEEE Sensors **3** (2004) 1534.
7 V. J. Lumelsky, M. S. Shur and S. Wagner: IEEE Sensors J. **1** (2001) 41.
8 S. Ito and H. Kawasaki: Proc. IEEE/RSJ Int. Conf. Intelligent Robots and Systems (Takamatsu, 2000) p. 1340.
9 L. Wang, and D. J. Beebe: Sens. Actuators A **84** (2000) 33.
10 L. Wang and D. J. Beebe: IEEE Trans. Biomed. Eng. **45** (1998) 151.
11 J. H. Shan, M. Mei, L. Sun, D. Y. Kong, Z. Y. Zhang, L. Ni, M. Meng and J. R. Chu: Proc. IEEE/RSJ Int. Conf. Intelligent Robots and Systems (Alberta, 2005) p. 1818.

12 F. Jiang, G.-B. Lee, Y.-C. Tai and C.-M. Ho: Sens. Actuators A **79** (2000) 194.
13 J. Engel, J. Chen and C. Liu: J. Micromech. Microeng. **13** (2003) 359.
14 H.-K. Lee, S.-I. Chang, and E. Yoon: J. Microelectromech. System **15** (2006) 1681.
15 E.-S. Hwang, J. Seo, and Y.-J. Kim: J. Microelectromech. System **16** (2007) 556.
16 R. F. Santos, R. F. Rocha, S. Lanceros-Mendez, C. Santos and J. G. Rocha: Proc. IEEE Int. Symp. Industrial Electronics (Dubrovnik, 2005) 1539.
17 K. L. Johnson: Contact Mechanics (Cambridge University Press, New York, 1994) p. 45.
18 Y.-J. Kim and M. G. Allen: IEEE Trans. Component Packaging Tech. **22** (1999) 282.
19 J. M. Gere and S. P. Timoshenko: Mechanics of Materials (PWS Publishing Company, Boston, 1997) p. 303.
20 J. Engel, J. Chen and C. Liu: App. Phys. Lett. **89** (2006) 221907.
21 E.-S. Hwang, Y.-J. Kim and B.-K. Ju: Sens. Acutators A **111** (2004) 135.
22 R. J. Young and P. A. Lovell: Introduction to Polymers (Chapman & Hall, London, 1994) p. 344.
23 J. E. Mark and B. Erman: Rubberlike Elasticity (Cambridge University Press, Cambridge, 2007) p. 61.
24 E. M. Arruda and M. C. Boyce: J. Mech. Phys. Solid **41** (1993) 389.